Highlights in Art and Design
ISSN: 2957-8787 | Vol. 13, No. 2, 2026

Design and Efficacy Evaluation of an Ergonomics Office Chair Intelligent Support System Based on Back Pressure Sensin

Liya Jin *

School of Design and Architecture, Zhejiang University of Technology, Hangzhou, Zhejiang, China

* **Corresponding author:** Liya Jin

Abstract: To address lower back fatigue and poor sitting posture associated with prolonged office work, this study developed an intelligent office chair support system based on back pressure sensing. The system utilizes a matrix of back pressure sensors to continuously monitor pressure distribution. This data guides the adaptive adjustment of zoned air-cells and a low-cost sliding backrest mechanism, working together to provide personalized support for the physiological curvature of the spine during dynamic sitting postures. A controlled experiment was conducted, comparing the prototype against commercially available chairs rated for high and low comfort using surface electromyography and subjective comfort ratings. The results show that the intelligent seat significantly delayed fatigue in the erector spinae muscle ($p < 0.05$) and effectively reduced lower back discomfort. This confirms its effectiveness in optimizing sitting posture load distribution, enhancing comfort, and improving anti-fatigue performance. The study offers a new direction for ergonomic design in office seating.

Keywords: Intelligent Office Chair; Back Pressure Sensing; Zoned Air-cell Support; Muscle Fatigue; Ergonomics.

1. Introduction

Sedentary office work is a widespread issue, with studies indicating that prolonged sitting significantly elevates the risk of musculoskeletal pain [1] and may lead to conditions such as lower back pain and lumbar disc herniation. The core progression involves: firstly, sustained static sitting causes static fatigue in the lumbar and back muscles [2]; secondly, muscle fatigue reduces support capacity, leading to poor posture and biomechanical imbalance of the spine [3]; thirdly, abnormal spinal curvature results in uneven pressure on intervertebral spaces, causing disc deformation and nerve compression, which manifests as soreness, numbness, and swelling in the lower limbs [4].

Current research primarily focuses on two approaches. The first involves alternating between sitting and standing to alleviate muscle fatigue, with recommended sit-stand ratios ranging from 1:1 to 3:1 [5]. This approach has been shown to reduce lower back discomfort [6][7], although related products such as active office chairs may affect work efficiency [8]. The second approach aims to extend muscle fatigue duration and assist in maintaining the physiological curvature of the spine through scientifically designed upper body support. The natural physiological curvature of the spine in an upright posture is generally regarded as a relatively healthy and reasonable alignment [9][10]. Effective support design should provide adequate back support while encouraging the maintenance of a healthy spinal curvature. The lumbar region, being the most loaded and mobile transitional segment [11], has become a focal point in support design. Studies confirm that lumbar support reduces spinal load [12], and maintaining lumbar lordosis is also crucial for minimizing load [13]. In seat design, lumbar support is often considered central to backrest optimization [14]. Consequently, most ergonomic chairs commonly feature a prominent lumbar support design, as illustrated in Figure 1.

Figure 1. Ergonomic Chair

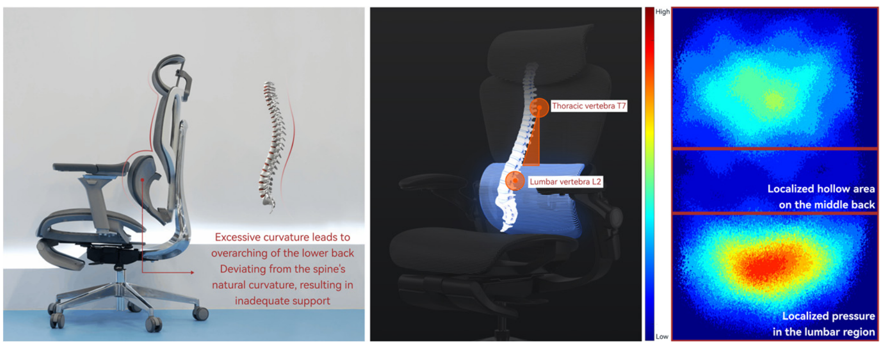

Figure 2. Illustration of Excessive Arching of the Lower Back

However, excessive emphasis on lumbar protrusion can easily lead to separation of the upper back from the chair backrest, causing posterior displacement of the thoracic spine and forward head posture, ultimately resulting in kyphosis [15]. Concurrently, high-pressure zones form in the lumbar region, as shown in Figure 2, which can exacerbate ischemic fatigue in soft tissues [16].

On the other hand, office sitting postures are dynamic, with a reclining angle between 110°and 135°being a common preference [17]. However, during reclining, the misalignment between the hip joint's center of rotation and the chair's pivot axis generates shear forces, leading to the "back-scrubbing effect" [18]. Existing solutions, such as fixed pivot points or synchronous tilt mechanisms [19], often involve complex structures and high costs, posing limitations that hinder widespread adoption.

This study posits that the key lies in providing scientifically sound back support across various sitting postures to maintain a healthy physiological spinal curvature. The design concept aims to achieve balanced pressure distribution across the entire spine statically, offering personalized and precise support. Dynamically, it seeks to employ a low-cost, simple mechanism that keeps the backrest support points relatively stationary relative to the characteristic points of the human spine during tilting, thereby achieving the goal of "zero back-scrubbing" and minimizing relative motion.

2. Sample Design

This study was designed based on the natural physiological curvature of the adult male spine. According to literature, the normal range of lumbar lordosis in males is approximately 20°–45° [20], with a mean value of about 32.42° ± 6.29° [21]. Thoracic kyphosis generally falls within 35°–45° [20]. Based on these data, lateral spinal radiographs of 24 adult males were collected and digitally processed to derive a representative physiological spinal curve. This curve informed the design of a standard backrest support panel made of ABS plastic (Figure 3). The panel features a graded wall thickness, gradually decreasing from 7 mm at the upper section to 4 mm at the lower section. The reduced thickness at the lower region enhances conformity and dynamic adaptability, while the increased thickness at the upper section improves bending stiffness to provide adequate shoulder and back support.

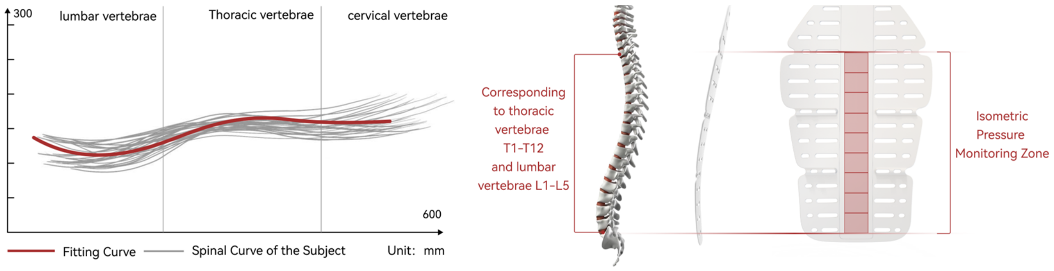

Figure 3. Fitted Curve and Support Panel

To finely regulate pressure distribution and cover spinal segments from T1–T12 in the thoracic region to L1–L5 in the lumbar region, the support surface was divided into three zones along the spine: upper, middle, and lower back. Each zone contains three pressure detection areas, resulting in a total of nine independent equally spaced regions where a matrix of thin-film pressure sensors was placed. The backrest inclination angle θ (90°–150°) was introduced as the independent variable, and multidimensional pressure data were collected. Ten healthy adult male participants were invited to perform sitting trials at four typical recline angles: 90°, 110°, 130°, and 150°, during which real-time pressure at each detection point was recorded. Considering the influence of body weight on absolute pressure values, the study adopted the normalized Pressure Ratio Coefficient as the key control parameter.

The pressure value measured at each point (P_i) is divided by the participant's body weight(W), to obtain the Normalized Pressure Ratio Coefficient (PRC). That is:

$$PRC_i(\theta) = \frac{P_{i(\theta)}}{W} \times 100\% \quad (1)$$

Here,P_i represents the pressure at the i-th measurement point, and W denotes the body weight. The distribution patterns of PRC across measurement points under varying angles and postures were identified through analysis of multiple experimental datasets.Statistical analysis was performed on experimental data collected from multiple subjects. Following the removal of outliers, the average ratio coefficient PRC_i was calculated for each measurement point under different tilt angles and postures. The resulting set $\{P\bar{R}C_1, P\bar{R}C_2, \dots, P\bar{R}C_{10}\}$ serves as the target benchmark for the system to assess the healthy support state.Based on the established pressure ratio benchmark, nine airbag actuator units were integrated behind the backrest support panel to form a dynamic support mechanism driven by pressure-compensation, as illustrated in Figure 4. A closed-loop feedback control system was designed to regulate the inflation and deflation of this multi-airbag array, enabling active adaptive support for the user's spinal alignment.

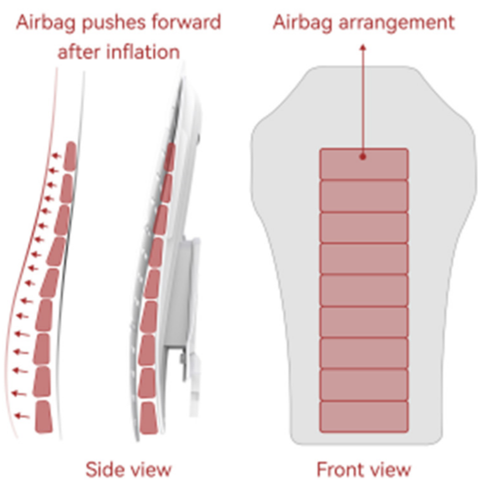

Figure 4. Schematic Diagram of Airbag Assembly

During the system initialization phase, the current user's body weight W_{user} is manually entered. The system then proceeds to the posture recognition stage, where it identifies the user's current backrest inclination angle $\theta_{current}$ based on data from a backrest angle sensor and an analysis of the pressure distribution pattern. According to this angle, the corresponding set of ideal pressure ratio coefficients $\{P\bar{R}C_{i\_target}\}$ is retrieved from a pre-established database. Subsequently, the theoretical target pressure P_{i_target} for each support zone is calculated using the following equation:

$$P_{i_{target}} = P\bar{R}C_{i_{target}} \times W_{user} \quad (2)$$

In the real-time monitoring and error analysis stage, the system continuously acquires the actual pressure P_{i_actual} in each zone via sensors and calculates the deviation from the target value:

$$\Delta P_i = P_{i_{target}} - P_{i_{actual}} \quad (3)$$

Finally, in the adjustment and execution stage, a permissible error threshold ϵ is defined. The pressure deviation ΔP_i for each zone is evaluated. If $|\Delta P_i| \leq \epsilon$, the air pressure in the corresponding airbag remains unchanged. If $\Delta P_i > \epsilon$, it indicates insufficient support, and the control system inflates the respective airbag. Conversely, if $\Delta P_i < -\epsilon$, it signals localized excessive pressure, prompting the system to deflate that airbag. This process enables adaptive adjustment of the support.

On another front, to reduce back shear forces caused by the misalignment of pivoting axes between the user and the chair during reclining, this study proposes a low-cost sliding-back mechanism integrated with the seat frame. Kobara et al. [22] demonstrated that mechanical assistance can promote coordinated motion between the user and the chair, thereby lowering shear forces. Building on this, the present study designed a more streamlined and efficient linkage solution (Figure 5). Its core consists of a pulley-and-rail mechanism housed inside the back frame. When the user reclines, the seat base drives the back frame to tilt rearward, while pressure from the back and gravity cause the pulley to slide downward along the rail. This motion compensates for the difference in rotational arc between the torso and the backrest, synchronizing the movement of the user and the chair. As a result, the contact points between the back and the backrest remain relatively stable throughout the reclining process.

Figure 5. Sliding Back Component and Backrest Movement Description

Based on the design of the support panel, the sliding-back mechanism, and the integrated air-cell adjustment system, a functional prototype was developed and assembled. The physical prototype is shown in Figure 6 and will serve as the experimental seat for subsequent performance evaluation and validation.

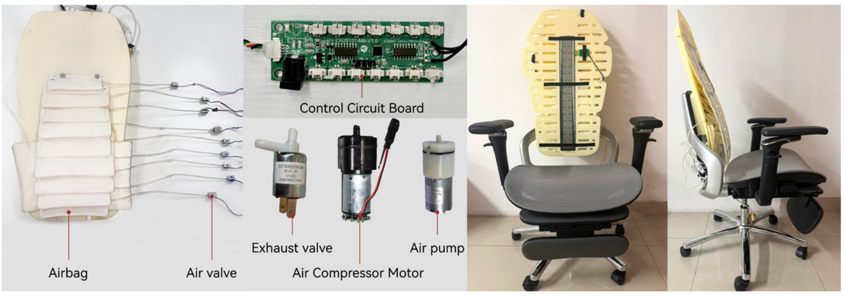

Figure 6. Physical Sample

3. Experimental Design

To validate the effectiveness of the proposed dynamic sliding-back structure and the three-zone air-cushion support system, a comparative experiment was conducted. First, control chairs were selected based on market representativeness and functional comparability. Experts identified seven chair models from a pool of office chairs that ranked within the top 20% in sales on Taobao over the past year, fell within a comparable price range, and featured zoned support and motion-compensation mechanisms (Figure 7). These chairs represent the current industry benchmark for dynamic support and pivot compensation.

Each evaluator sat in every chair for 8 minutes and then immediately completed a subjective comfort questionnaire, rating back, lumbar, and overall comfort on a 5-point Likert scale (1 = “very uncomfortable”, 5= “very comfortable”). The statistical results (Table 1) showed the following overall comfort ranking from highest to lowest: G, E, D, C, F, A, B.

The chairs with the highest (G) and lowest (B) comfort ratings were ultimately selected as control groups. This approach helps to amplify the differences in lumbar and back muscle activity between the new prototype and existing products, avoiding the performance-neutralizing effect of moderately comfortable chairs. It also allows for evaluating the new chair in two aspects: reducing biomechanical load (compared to the low-comfort chair) and enhancing overall comfort (compared to the high-comfort chair), thereby providing a scientific assessment of sitting posture improvement. The formal experiment adopted a mixedmethod design, combining subjective and objective measures. Eight healthy male graduate students participated as subjects in a repeated-measures study comparing the prototype (featuring zoned air-cushion support) with the selected high- and low-comfort market chairs. Surface electromyography (sEMG) was used to analyze muscle activity: the root mean square (RMS) value was employed to quantify static muscle load, while the decline rate of the median power frequency (MPF) served to assess muscle fatigue accumulation during prolonged sitting [23].

Table 1. Mean Subjective Comfort Evaluation Scores for A-G Seat Samples

Seat Model	Back comfort (Mean±SD)	Waist comfort (Mean±SD)	Overall comfort (Mean±SD)
A	2.2±0.79	2.3±0.82	2.5±0.85
B	2.2±0.92	1.6±0.70	1.9±0.74
C	3.2±1.03	3.2±0.92	3.0±1.05
D	3.3±0.82	3.6±0.84	3.4±0.97
E	3.0±1.15	4.3±0.67	3.6±0.84
F	3.2±0.79	3.2±0.92	3.0±0.82
G	3.7±0.82	4.6±0.52	4.2±0.63

3.1. Methods

The study involved eight male graduate students (aged 23±1 years, height 1.76±0.02 m, body weight 70.7±7.1 kg, BMI 24.2±1.3 kg/m²) with no history of chronic low back pain, spinal or pelvic surgery, lower limb surgery, neuromuscular disorders, or skin sensitivity that could affect postural stability. The study protocol was approved by the Ethics Committee, and all participants provided written informed consent.

Three office chairs were evaluated: an experimental chair (A) equipped with a novel air-cushion zoned backrest, a commercially available chair rated highly for comfort (B), and a commercially available chair rated low in comfort (C)—the latter two selected based on prior Likert scale ratings. To control for initial force deviations due to individual anatomical differences, all chairs were individually adjusted in seat height and depth according to each participant's anthropometric measurements, ensuring an equivalent initial biomechanical support condition.

Participants were assigned to the three chair conditions in a randomized order following a standard Latin square design. Each testing session included two seated postures performed sequentially: (1) an upright sitting posture, with the trunk held straight in a standardized 90° position, and (2) a reclined sitting posture, in which the body leaned back against the chair backrest at an approximate angle of 120° (Sun Xinxin et al., 2014) [18], as illustrated in Figure 7.

Figure 7. Seats and Seating Positions in the Experiment

Each participant completed a total of six experimental sessions (3 chairs × 2 postures). Each seated posture was maintained over a period of 45 minutes, with a 10-minute rest interval between sessions. To obtain stable postural data and minimize interference from fatigue, all measurements were taken 30 minutes after the beginning of each sitting session.

3.2. Data Collection and Processing

Muscle activity was monitored using a BIOPAC MP150 multiphysiological recording system. Prior to electrode placement, the skin was shaved, lightly abraded, and cleaned with alcohol. Surface electrodes (10 mm in diameter, 20 mm inter-electrode distance) [24] were positioned over the muscle bellies of the left and right erector spinae (LES, 3 cm lateral to the L3 spinous process), multifidus (MF, 2 cm lateral to the L5 spinous process), and quadratus lumborum (QL, 4 cm lateral to the erector spinae). These muscles represent a core functional unit for lumbar stability, primarily responsible for postural control, segmental stabilization, and lateral balance, respectively. Monitoring their activity provides insight into biomechanical homeostasis during prolonged sitting [25][26][27]

Subjective discomfort in the upper back and lower back (lumbar region) was recorded after each session using the Borg CR-10 scale, where 0 indicates no discomfort and 10 represents extreme discomfort. Electromyographic (EMG) signals were sampled at 1000 Hz. Raw surface EMG data were band-pass filtered at 30–450 Hz to reduce noise, and a 50 Hz notch filter was applied to eliminate mains interference. All data processing was performed in MATLAB R2024b.

4. Results and Discussion

4.1. Objective Results Analysis

As shown in Table 2, muscle activation was generally higher during upright sitting compared to reclined sitting, indicating that sitting posture influences the baseline load on the lumbar and back muscles. Under the higher-load upright condition, the experimental chair showed a trend toward reduced muscular effort, with the mean RMS value of the erector spinae lower than that observed in both control chairs. Although ANOVA indicated that this difference did not reach statistical significance ($P = 0.085$), the decrease in the mean value suggests that the air-cushion zoned support physically offloaded part of the spinal burden.

In the reclined posture, where trunk weight is transferred to the backrest, the differences in RMS values among the chairs diminished further. The RMS of the quadratus lumborum and multifidus muscles showed little variation across conditions, indicating that these muscles primarily contribute to postural fine-tuning and deep stabilization during static sitting and are less sensitive to changes in external support structures.

Table 2. RMS Statistics Table

Muscle	Seated position	Control group-Low (Mean±SD)	Control group- High (Mean±SD)	Experimental group (Mean±SD)	F	P
ES	Upright	0.112±0.088	0.118±0.092	0.082±0.075	2.94	0.085
	Recline	0.104±0.108	0.062±0.084	0.071±0.089	2.15	0.153
QL	Upright	0.081±0.095	0.092±0.108	0.074±0.088	0.72	0.503
	Recline	0.052±0.082	0.061±0.091	0.055±0.084	0.12	0.887
MF	Upright	0.015±0.012	0.014±0.011	0.012±0.009	0.56	0.583
	Recline	0.008±0.006	0.009±0.007	0.011±0.010	0.85	0.448

(Note: *Indicates a significant difference compared to the control group ($p < 0.05$)

The mean power frequency (MPF) slope serves as a key frequency-domain indicator for assessing muscular fatigue accumulation. Values closer to zero or positive values (an upward trend) reflect better anti-fatigue performance. In terms of fatigue resistance, the experimental chair demonstrated statistically meaningful outcomes.

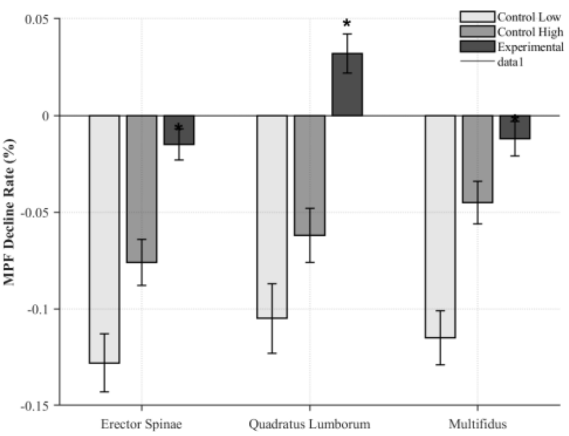

Figure 8. MPF Statistics in an Upright Sitting Posture

As illustrated in Figure 8, during the upright sitting task, the low-comfort control chair exhibited a clear leftward shift in the power spectrum, suggesting the onset of muscle fatigue. In contrast, the experimental chair showed MPF slopes that approached zero in both the erector spinae and quadratus lumborum muscles, with a slight positive increase observed in the quadratus lumborum (0.032 ± 0.02). These findings indicate that the air-cushion zoned support system offers more sustained physiological benefits compared to traditional chair designs, primarily by dynamically maintaining the lumbar curvature and preventing localized muscular overload.

Based on the analysis of experimental data from the three target muscle groups in the back (erector spinae, multifidus, and quadratus lumborum), this study found that the air-cushion zoned support system in the experimental chair demonstrated a significant anti-fatigue effect on the erector spinae ($p < 0.05$), as shown in Table 3. In contrast, biomechanical differences across the three chairs were minimal for the multifidus—which maintains deep stabilization—and the quadratus lumborum, responsible for lateral balance, with no statistically significant variations observed.

Table 3. Statistical Results of Electromyographic Indicators for the Erector Spinae (ES) Under Different Seating Conditions (n=8)

Experimental Conditions	Evaluation Indicators	Control group-Low (Mean±SD)	Control group-High (Mean±SD)	Experimental group (Mean±SD)	F	P
Recline	RMS	0.10±0.11	0.06±0.08	0.07±0.09	2.15	0.153
	MPF	-0.05±0.12	-0.09±0.14	-0.01±0.08	4.82	0.024*
Upright	RMS	0.10±0.09	0.11±0.09	0.08±0.08	2.94	0.085
	MPF	-0.01±0.09	-0.05±0.08	0.01±0.04	5.11	0.019*

(Note: *Indicates a significant difference compared to the control group ($p < 0.05$)

The key finding of this study is that the experimental seat showed a significantly lower rate of decline in MPF for the erector spinae muscle compared to the control ($p < 0.05$). Under both seated postures tested, the MPF decline rate in the experimental group was close to zero or even exhibited a positive regression, indicating that the dynamic sliding backrest mechanism combined with zoned air-cell support effectively mitigated muscle fatigue. The erector spinae, a superficial core muscle group [28], is sensitive to displacement of the supporting surface. In the experimental seat, the sliding backrest compensated for axis misalignment during backward leaning, thereby eliminating defensive muscle contraction caused by "back shear." Meanwhile, the dynamic zoned air-cell support filled the gaps in load distribution at the lumbosacral region, precisely offloading the erector spinae. This shift from passive adaptation to active support forms the biomechanical basis for delaying fatigue in the erector spinae.

Although the RMS mean values in the experimental group showed a declining trend, some differences did not reach statistical significance (e.g., $p = 0.085$ for the erector spinae in the upright posture). This may be due to the fact that seated posture maintenance involves both the erector spinae and deeper muscles such as the multifidus. When external support shares part of the load, motor units may remain somewhat activated to preserve fine balance.

Furthermore, differences among the three seat types were minimal regarding the multifidus and quadratus lumborum muscles. The multifidus primarily maintains intersegmental stability of the spine, and its activation depends more on the intrinsic mechanical state of the spine than on external support morphology. The quadratus lumborum is more engaged in lateral stabilization; its coronal plane support role was not fully elicited in this experiment, which was primarily conducted in the sagittal plane.

4.2. Subjective Outcome Analysis

The Borg CR-10 scale data submitted by participants were analyzed to evaluate changes in back discomfort across different seats and postures, as summarized in Table 4.

Table 4. Scores for Localized Body Discomfort Under Different Seating Positions and Chair Conditions (Mean ± SD, n=8)

Body part	Seated position	Control group-Low (Mean±SD)	Control group-High (Mean±SD)	Experimental group (Mean±SD)	P (Seat Effect)
lower back	Recline	5.2±1.4	4.1±1.1	2.6±0.9	<0.001**
	Upright	4.5±1.2	3.2±0.9	2.0±0.7	0.003*
Upper back	Recline	2.8±1.1	2.5±1.0	2.3±0.8	0.312
	Upright	2.1±0.9	1.8±0.7	1.9±0.8	0.455

(Note: *Indicates a significant difference compared to the control group ($p < 0.05$)

Subjective ratings indicated that all participants reported higher overall discomfort in the upright sitting posture compared to the reclined posture, suggesting that the backrest shared part of the trunk load in the reclined position, thereby alleviating perceived pressure. In upright sitting, the experimental seat demonstrated the most pronounced advantage, with a score (2.6±0.9) approximately 50% lower than that of the comfort control group. This aligns with the physiological observation of the most stable MPF in the erector spinae, confirming that the zoned air-cell support translates into measurable comfort improvement. Although lower back discomfort ratings were significantly higher than upper back ratings in both postures, the experimental seat reduced this discrepancy, promoting more balanced load distribution across the back.

The experimental seat maintained the lowest discomfort levels in both postures, demonstrating robustness in dynamic office scenarios. Notably, no significant differences were observed among the three seats in terms of upper back discomfort. This may be due to the fact that the thoracic region did not reach a fatigue threshold within the short experimental period (45 minutes). Alternatively, it may suggest that the current stiffness ratio of the upper back air-cells could be further optimized; adjusting their firmness in future designs may help balance pressure distribution across the entire back.

5. Conclusion

This study employed an integrated objective-subjective approach to evaluate the biomechanical performance of a novel seat featuring zoned air-cell support. The following conclusions were drawn:

1. The intelligent zoned air-cell support demonstrates significant physiological anti-fatigue benefits. During prolonged static sitting, the experimental seat significantly delayed the fatigue progression of the erector spinae muscle ($p < 0.05$). This suggests that the design does not merely reduce overall muscle activation but enhances the metabolic efficiency of core muscles in maintaining posture by optimizing lumbar pressure distribution.

2. Subjective perception aligns closely with physiological indicators. Ratings on the Borg CR-10 scale indicated that the experimental seat significantly reduced subjective discomfort in the lower back. The improvement in perceived comfort corresponds with the objective reduction in electromyographic fatigue rates, confirming the practical effectiveness of the design.

In summary, this study verifies that an intelligent air-cell adjustment system based on pressure-distribution monitoring can actively intervene biomechanically in sitting behavior. It encourages users to maintain a healthy spinal curvature unconsciously, thereby promoting the long-term habituation of correct posture. This design offers a more physiologically adaptive dynamic support solution, providing a theoretical basis for preventing occupational musculoskeletal disorders and optimizing office furniture design. Future research will further validate the general applicability of this system across broader populations.

References

[1] Daniel P Bailey. Sedentary behaviour in the workplace: prevalence, health implications and interventions. British Medical Bulletin. 2021; Volume 137, Issue 1, March, Pages 42–50.

[2] Jung, K.-S., Jung, J.-H., In, T.-S., Cho, H.-Y. Effects of Prolonged Sitting with Slumped Posture on Trunk Muscular Fatigue in Adolescents with and without Chronic Lower Back Pain. Medicina. 2021; 57, 3.

[3] XIONG Kai-wen, WANG Yao, CHENG Shan, ZHANG Tai-hui, CONG Lin, HU Wen-dong. Study on Lumbar Muscle Contraction in the Sitting Positions with Different Anteroposterior Inclination of the Spine Based on Surface Electromyography. Progress in Modern Biomedicine. 2021; Vol.21 NO.24.

[4] Liu T, Wang Y, Xu Z, Wu T, Zang X, Li M, Li J. Application study of 3D LAVA-Flex on lumbar intervertebral disc degeneration. Eur J Med Res. 2021 May 7;26(1):43.

[5] Karakolis T, Callaghan JP. The impact of sit-stand office workstations on worker discomfort and productivity: a review. Applied Ergonomics. 2014 May;45(3):799-806.

[6] Chambers AJ, Robertson MM, Baker NA. The effect of sit-stand desks on office worker behavioral and health outcomes: A scoping review. Applied Ergonomics. 2019 Jul; 78: 37-53.

[7] Bao S, Lin JH. An investigation into four different sit-stand workstation use schedules. Ergonomics. 2018 Feb;61(2):243-254.

[8] Mamiko Noguchi, Jackie D. Zehr, Liana M. Tennant, Donna J. Fok, Jack P. Callaghan, Increasing movement during office work at sit-stand workstations: A novel seating device to facilitate transitions. Applied Ergonomics,2023, Volume 111, 104044.

[9] Persson, E., Zetaruk, M. Swimming and the Spine. In: Micheli, L., Stein, C., O'Brien, M., d' Hemecourt, P. (eds) Spinal Injuries and Conditions in Young Athletes. Contemporary Pediatric and Adolescent Sports Medicine., New York: Springer; 2014.

[10] Moreira R, Teles A, Fialho R, Baluz R, Santos TC, Goulart-Filho R, Rocha L, Silva FJ, Gupta N, Bastos VH, et al. Mobile Applications for Assessing Human Posture: A Systematic Literature Review. Electronics. 2020; 9(8):1196.

[11] Zeng Zhongyou. Infinite thinking, bounded actions, actively and steadily carrying out minimally invasive lumbarfusion technology. Spinal Surg. 2023; 21(4):220-223.

[12] Andersson BJ, Ortengren R, Nachemson A, Elfström G. Lumbar disc pressure and myoelectric back muscle activity during sitting. I. Studies on an experimental chair. Scand J Rehabil Med. 1974;6(3):104-14.

[13] Cho IY, Park SY, Park JH, Kim TK, Jung TW, Lee HM. The Effect of Standing and Different Sitting Positions on Lumbar Lordosis: Radiographic Study of 30 Healthy Volunteers. Asian Spine J. 2015; 9(5):762-9.

[14] FAN Qinhong, JIANG Xingchen,WU Xueliang,NIE Min,XIN Yunsheng, LI Haolin, JIA Xianyu. Experimental Research on Optimization Design and Comfortof Locomotive Seat Based on Ideal Pressure. JOURNAL OF MECHANICAL ENGINEERING. 2022; 58(10):383-394.

[15] Singla D, Veqar Z. Association Between Forward Head, Rounded Shoulders, and Increased Thoracic Kyphosis: A Review of the Literature. Journal of Chiropractic Medicine. 2017;16(3):220-229.

[16] Akgunduz A, Rakheja S , Tarczay A .Distributed occupant-seat interactions as an objective measure of seating comfort. International Journal Of Vehicle Design. 2014; 65(4):293.

[17] SUN Xinxin, ZHOU Di, JIANG Bin, XU Boming. Clustering analysis of sitting posture on office chair. Journal of Forestry Engineering. 2018; 3(05):158-164.

[18] Goossens RH, Snijders CJ. Design criteria for the reduction of shear forces in beds and seats. J Biomech. 1995; 28(2):225-30.

[19] Chang Y, Kang J, Jeong B, Kim Y, Hong E-P, Kim G. Analysis of Body-Slip and Buttock Pressure Characteristics during Operation of a Double-Sliding Reclining Wheelchair in Patients with Spinal Cord Injury. Applied Sciences. 2021; 11(22):10651.

[20] Castillo, E. and Obregón, R. Assessment of the sagittal spinal curvatures in dancers of Spanish dance. Journal of human sport and exercise. 2018;13(1).

[21] Abrisham SMJ, Ardekani MRS, Mzarch MAB. Evaluation of the Normal Range of Thoracic Kyphosis and Lumbar Lordosis Angles Using EOS Imaging. Maedica (Bucur). 2020; 15(1):87-91.

[22] Kobara K, Nagata Y, Takahashi H, Osaka H, Suehiro T, Fujita D. Effect of fluctuation in the parallel force exerted on the buttocks on discomfort during sitting in experimental ergonomic chair with tilt-in-space and reclining functions. Prosthet Orthot Int. 2025. Epub ahead of print. PMID: 40763 266.

[23] ZHU Rongxin. A Study of Lumbar Muscle Fatigue of Combine Harvester Drivers Based on sEMG. Industrial Engineering Journal. 2020; 23(1):119-125.

[24] Amiri B, Zemková E. Fatigue and recovery-related changes in postural and core stability in* sedentary employees: a study protocol. Front Physiol. 2024; 15:1490041.

[25] Bastos de Oliveira V, Albuquerque Brandão MC, Coelho de Albuquerque Pereira W, Fernandes de Oliveira L. Lumbar multifidus layers stiffness at L5-S1 level in prone and sitting posture measured by shear wave elastography. J Back Musculoskelet Rehabil. 2024; 37(5):1241-1248.

[26] Desgagnés A, Desmons M, Cyr JP, Simoneau M, Massé-Alarie H. Motor Responses of Lumbar Erector Spinae Induced by Electrical Vestibular Stimulation in Seated Participants. Front Hum Neurosci. 2021; 15:690433.

[27] López-Redondo M, Vicente-Campos D, Álvarez-González J, Roldán-Ruiz A, Sánchez-Jorge S, Buffet-García J, Rabanal-Rodríguez G, Valera-Calero JA. Association of Quadratus Lumborum Muscle Stiffness with Chronic Low Back Pain Features: An Observational Study. Medicina. 2025; 61(2):270.

[28] Xu Hongmei, Wang Qichao, Zhang Wenjie, et al. Optimization of tractor seat position parameters based on biomechanicalcharacteristics. Transactions of the Chinese Society of Agricultural Engineering (Transactions of the CSAE). 2022; 38(22): 32-40.